Article

Planar Chiral Azobenzenophanes as Chiroptic Switches for Photon Mode Reversible Reflection Color Control in Induced Chiral Nematic Liquid Crystals

Manoj Mathews, and Nobuyuki Tamaoki

J. Am. Chem. Soc., **2008**, 130 (34), 11409-11416 • DOI: 10.1021/ja802472t • Publication Date (Web): 02 August 2008

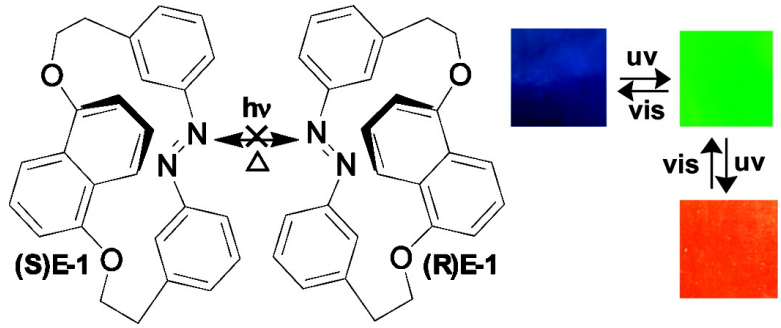

More About This Article

Additional resources and features associated with this article are available within the HTML version:

- Supporting Information
- Access to high resolution figures
- Links to articles and content related to this article
- Copyright permission to reproduce figures and/or text from this article

View the Full Text HTML

J|A|C|S
ARTICLES

Published on Web 08/02/2008

Planar Chiral Azobenzenophanes as Chiroptic Switches for Photon Mode Reversible Reflection Color Control in Induced Chiral Nematic Liquid Crystals

Manoj Mathews and Nobuyuki Tamaoki*

Molecular Smart System Group, Nanotechnology Research Institute, National Institute of Advanced Industrial Science and Technology (AIST), 1-1-1, Higashi, Tsukuba, Ibaraki 305-8565, Japan

Received April 4, 2008; E-mail: n.tamaoki@aist.go.jp

Abstract: In this report, for the first time, a planar chiral photoresponsive compound has been employed in commercially available nematic liquid crystals to achieve phototunable reflection colors. We designed an azobenzenophane compound having conformational restriction on the free rotation of naphthalene moiety to impose an element of planar chirality and the corresponding enantiomers were resolved by HPLC on chiral column. We have determined the absolute configuration by comparison of density functional theory (DFT) calculations of its electronic circular dichroism (ECD) spectrum and specific rotation $[\alpha]_D$ to experimental ECD and $[\alpha]_D$ data. Enantiomers exhibit photochemically reversible isomerization in solution without undergoing thermal or photoinduced racemization. As chiroptic switches in different host nematic liquid crystals, they exhibit good solubility, moderately high helical twisting power, as well as a large change in helical twisting power due to photoisomerization. A unique feature of these chiral photochromic compounds is that no other auxiliary chiral agents is required to achieve a fast photon mode reversible full-range color control in induced cholesterics, that is, both the hypsochromic and bathochromic shift can be obtained from a single LC formulation by reversible photoisomerization of the single chiral compound.

Introduction

Stimuli responsive chiral self-assembling architectures are of key importance to the existence of life in nature and continue to emerge as the primary building blocks for the design of various functional nanoscale assemblies.[1] Of particular interest are the macromolecular and supramolecular systems possessing chiral photochemical molecular switches because it offers the advantage of using light as the external stimuli to reversibly control the molecular and supramolecular chirality.[2] For example, reversible helical self-assembly of chiral nematic liquid crystals that reflect specific wavelength of light associated with its helical pitch are at the forefront in the development of optoelectronic devices[3] and modern color information technology[4] and continue to stimulate innovative research in view of other possible biomedical applications.[5] Most of these applications have in common the necessity to obtain tunable helical pitch in response to light coupled with other external parameters such as temperature and electric and magnetic fields and to the exposure of dopants. Our interest in this topic is for the design of full-color recording devices that allow quick photon mode rewritable imaging. In recent years, we have demonstrated that thermally stable light driven full color recording is possible by doping the glass forming chiral nematic liquid crystal with achiral photochromic azobenzene derivatives.[6] Alternatively, a chiral photoresponsive dopant can act as both a chiral agent to induce a chiral nematic phase in a nematic liquid crystal and a photoresponsive moiety to control the helical pitch through photo isomerization.[7] When a chiral solute is dissolved in nematic liquid crystal at the limit of low concentration, the induced pitch P is correlated with the weight concentration C_w

(1) (a) *Molecular Motors*; Schliwa, M., Ed.; Wiley-VCH: Weinheim, 2003. (b) Kelly, T. R. *Molecular Devices and Machines: A Journey into the Nanoworld*; Balzani, V., Venturi, M., Credi, A., Eds.; Wiley-VCH: Weinheim, 2003. (c) Tang, K.; Green, M. M.; Cheon, K. S.; Selinger, J. V.; Garetz, B. A. *J. Am. Chem. Soc.* **2003**, 7313–7323. (d) Kinbara, K.; Aida, T. *Chem. Rev.* **2005**, *105*, 1377–1400.

(2) (a) *Molecular Switches*; Feringa, B. L., Ed.; Wiley-VCH: Weinheim, 2001. (b) Li, J.; Schuster, G. B.; Cheon, K. S.; Green, M. M.; Selinger, J. V. *J. Am. Chem. Soc.* **2000**, *122*, 2603–2612. (c) Mayer, S.; Zentel, R. *Macromol. Rapid Commun.* **2000**, *21*, 927–930. (d) Eelkema, R.; Pollard, M. M.; Katsonis, N.; Vicario, J.; Broer, D. J.; Feringa, B. L. *J. Am. Chem. Soc.* **2006**, *128*, 14397–14407. (e) Hembury, G. A.; Borovkov, V. V.; Inoue, Y. *Chem. Rev.* **2008**, *108*, 1–73.

(3) (a) Collings, P. J.; Hird, M. *Introduction to Liquid Crystals: Chemistry and Physics*; Gray, G. W., Goodby, J. W., Fukuda, A., Eds.; Taylor & Francis Ltd.: London, 1997. (b) Chilaya, G. In *Chirality in Liquid Crystals*; Kitzerov, H.-S., Bahr, C., Eds.; Springer: New York, 2001. (c) Matharu, A. S.; Jeeva, S.; Ramanujam, P. S. *Chem. Soc. Rev.* **2007**, *36*, 1868–1880.

(4) Tamaoki, N. *Adv. Mater.* **2001**, *13*, 1135–1147.

(5) (a) *Liquid Crystals: Frontiers in Biomedical Applications*; Woltman, S. J., Jay, G. D., Crawford, G. P., Eds.; World Scientific: Hackensack, NJ, 2007. (b) Stewart, G. T. *Liq. Cryst.* **2003**, *30*, 541–557. (c) Hoogboom, J.; Clerx, J.; Otten, M. B. J.; Rowan, A. E.; Rasing, T.; Nolte, R. J. M. *Chem. Commun.* **2003**, *23*, 2856–2857. (d) Woltman, S. J.; Jay, G. D.; Crawford, G. P. *Nat. Mater.* **2007**, *6*, 929–938.

(6) (a) Tamaoki, N.; Song, S.; Moriyama, M.; Matsuda, H. *Adv. Mater.* **2000**, *12*, 94–97. (b) Mallia, V. A.; Tamaoki, N. *Chem. Soc. Rev.* **2004**, *33*, 76–84. (c) Akiyama, H.; Mallia, V. A.; Tamaoki, N. *Adv. Funct. Mater.* **2006**, *16*, 477–484. (d) Abraham, S.; Mallia, V. A.; Ratheesh, K. V.; Tamaoki, N.; Das, S. *J. Am. Chem. Soc.* **2006**, *128*, 7692–7698.

(7) (a) Ichimura, K. *Chem. Rev.* **2000**, *100*, 1847–1873. (b) Eelkema, R.; Feringa, B. L. *Org. Biomol. Chem.* **2006**, *4*, 3729–3745.

10.1021/ja802472t CCC: $40.75

of the dopant (weight of dopant/weight of solution) and its enantiomeric purity r according to the equation

$$P^{-1} = \beta C_w r \quad (1)$$

The proportionality constant β is referred to as the helical twisting power (HTP). Phototunable chiral dopants with not only high helical twisting power but also with large reversible change in HTP between its isomeric forms are prized. A great deal of effort has therefore been dedicated to the design of dopants incorporating photoresponsive moieties such as azobenzenes,[8] fulgides,[9] diarylethenes,[10] spiropyrans,[11] and overcrowded alkenes[12] with point, axial, and helical chirality. Accumulated experimental[7−12] and theoretical results[13] show that lower conformational freedom and higher structural rigidity of both dopant and the liquid crystalline host engender higher HTP values, whereas a large change in chiral conformations between the two distinct interconvertible forms of the chiroptic switch is desirable for achieving better phototunability of the helical pitch. In spite of the extensive research, reversible color control in induced cholesterics without added non photoresponsive chiral codopants is limited to recent reports employing helically chiral overcrowded alkenes[14] and axially chiral binaphthyl azobenzene derivatives.[8c,15] In both cases, a relatively slow thermal isomerization process of the dopants drives the reversibile bathochromic shift to the initial state, limiting their use in dynamic display- and variable color filter applications. Therefore, the discovery of new phototunable chiral dopants is important to broadening the utility of chiral nematic formulations. We report herein on a design for the first photoresponsive chiral dopant based on planar chirality and our success in fast photon mode reversible reflection color control over the entire visible region for the first time by employing these chiroptic switches as the only chiral additive in a commercially available nematic liquid crystalline host.

Although planar chirality is well-known in asymmetric reactions, catalysis, host−guest interactions,[16] and for the development of optically active liquid crystalline materials,[17] their employment as phototunable chiral dopants have so far not been explored. Recently, we first reported on planar chiral

Chart 1. Chemical Structure of the Planar Chiral Dopant **E-1** and the Space Filling Representations of the Corresponding Resolved Enantiomers

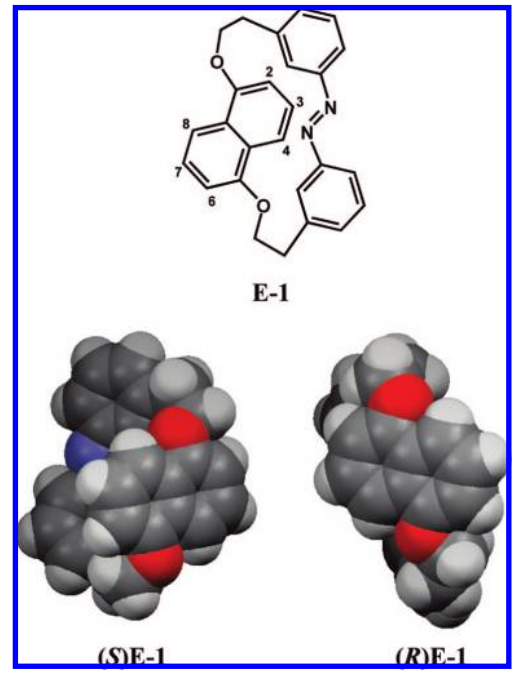

bicyclic azobenzene derivatives as efficient chiroptic switches with dynamic control over their racemization rate through *trans*−*cis* photoisomerization.[18] In the present study, we designed a small and rigid azobenzenophane consisting of a 1,5-dioxynaphthalene moiety with methylene linkages bonded at the meta positions of the photoresponsive unit. The incorporation of the 1,5-dioxynaphthalene ring system can impart an element of planar chirality to the molecule, provided there is no free rotation of naphthalene unit through the cavity of the macrocycle.[19] Molecular modeling indicated that bridges formed by two atoms (−CH_2−CH_2−) could impose planar chirality to such a molecule (Chart 1). Due to molecular constraints, the orientation of the two aromatic mesogenic core units (long molecular axis of naphthalene and azobenzene units) is expected to generate an inherent *twist* in the molecule, making them attractive as *twist agents* or potential chiral dopants in nematic solvents (Chart 2). The phototunability of helical twisting power of chiral dopants obtained by appending a photoresponsive azo moiety to an already existing point or axially chiral unit is

(8) (a) Ruslim, C.; Ichimura, K. *Adv. Mater.* **2001**, *13*, 37–40. (b) Pieraccini, S.; Masiero, S.; Spada, G. P.; Gottarelli, G. *Chem. Commun.* **2003**, 598–599. (c) Pieraccini, S.; Gottarelli, G.; Labruto, R.; Masiero, S.; Pandolini, O. S.; Spada, G. P. *Chem.−Eur. J.* **2004**, *10*, 5632–5639. (d) Yoshioka, T.; Ogata, T.; Nonaka, T.; Moritsugu, M.; Kim, S. N.; Kurihara, S. *Adv. Mater.* **2005**, *17*, 1226–1229. (e) Kawamoto, M.; Aoki, T.; Wada, T. *Chem. Commun.* **2007**, 930–932.
(9) (a) Janicki, S. Z.; Schuster, G. B. *J. Am. Chem. Soc.* **1995**, *117*, 8524–8527. (b) Yokoyama, Y.; Sagisaka, T. *Chem. Lett.* **1997**, 687–688.
(10) (a) Denekamp, C.; Feringa, B. L. *Adv. Mater.* **1998**, *10*, 1080–1082. (b) Yamaguchi, T.; Inagawa, T.; Nakazumi, H.; Irie, S.; Irie, M. *Chem. Mater.* **2000**, *12*, 869–871. (c) Yamaguchi, T.; Inagawa, T.; Nakazumi, H.; Irie, S.; Irie, M. *J. Mater. Chem.* **2001**, *11*, 2453–2458.
(11) Bossi, M. L.; Murgida, D. H.; Aramendia, P. F. *J. Phys. Chem. B* **2006**, *110*, 13804–13811.
(12) (a) Huck, N. P. M.; Jager, W. F.; de Lange, B.; Feringa, B. L. *Science* **1996**, *273*, 1686–1688. (b) Chen, C.-T.; Chou, Y.-C. *J. Am. Chem. Soc.* **2000**, *122*, 7662–7672. (c) van Delden, R. A.; Koumura, N.; Harada, N.; Feringa, B. L. *Proc. Natl. Acad. Sci. U.S.A.* **2002**, *99*, 4945–4949.
(13) (a) Gottarelli, G.; Hibert, M.; Samori, B.; Solladie, G.; Spada, G. P.; Zimmermann, R. *J. Am. Chem. Soc.* **1983**, *105*, 7318–7321. (b) di Matteo, A.; Todd, S. M.; Gottarelli, G.; Solladie, G.; Williams, V. E.; Lemieux, R. P.; Ferrarini, A.; Spada, G. P. *J. Am. Chem. Soc.* **2001**, *123*, 7842–7851. (c) Earl, E. J.; Wilson, M. R. *J. Chem. Phys.* **2003**, *119*, 10280–10288.
(14) Eelkema, R.; Feringa, B. L. *Chem. Asian J.* **2006**, *1*, 367–369.
(15) Li, Q.; Green, L.; Venkataraman, N.; Shiyanovskaya, I.; Khan, A.; Urbas, A.; Doane, J. W. *J. Am. Chem. Soc.* **2007**, *122*, 12908–12909.
(16) (a) Zanotti-Gerosa, A.; Malan, C.; Herzberg, D. *Org. Lett.* **2001**, *3*, 3687–3690. (b) Ma, Y.; Song, C.; Ma, C.; Sun, Z.; Chai, Q.; Andrus, M. B. *Angew. Chem., Int. Ed.* **2003**, *42*, 5871–5874. (c) Sato, I.; Ohno, A.; Aoyama, Y.; Kasahara, T.; Soai, K. *Org. Biomol. Chem.* **2003**, *1*, 244–246. (d) Gibson, S. E.; Knight, J. D. *Org. Biomol. Chem.* **2003**, *1*, 1256–1269. (e) Anderson, J. C.; Osborne, J. D.; Woltering, T. J. *Org. Biomol. Chem.* **2008**, *6*, 330–339.
(17) (a) Ziminsky, L.; Malthête, J. *Chem. Commun.* **1990**, 1495–1496. (b) Jacq, P.; Malthête, J. *Liq. Cryst.* **1996**, *21*, 291–293. (c) Chuard, T.; Cowling, S. J.; Ciurleo, M.F.-.; Jauslin, I.; Goodby, J. W.; Deschenaux, R. *Chem. Commun.* **2000**, 2109–2110. (d) Popova, E. L.; Rozenberg, V. I.; Starikova, Z. A.; Baumann, S. K-.; Kitzerow, H. -S.; Hopf, H. *Angew. Chem., Int. Ed.* **2002**, *41*, 3411–3414. (e) Brettar, J.; Burgi, T.; Donnio, B.; Guillon, D.; Klappert, R.; Scharf, T.; Deschenaux, R. *Adv. Funct. Mater.* **2006**, 260–267.
(18) Tamaoki, N.; Wada, M. *J. Am. Chem. Soc.* **2006**, *128*, 6284–6285.
(19) (a) Chang, M. H.; Masek, B. B.; Dougherty, D. A. *J. Am. Chem. Soc.* **1985**, *107*, 1124–1133. (b) Ballardini, R.; Balzani, V.; Becher, J.; Fabio, A. D.; Gandolfi, M. T.; Mattersteig, G.; Nielsen, M. B.; Raymo, F. M.; Rowan, S. J.; Stoddart, J. F.; White, A. J. P.; Williams, D. J. *J. Org. Chem.* **2000**, *65*, 4120–4126.

Chart 2. Schematic Representation Highlighting the Inherent Molecular "*Twist*" and the Switching Process in Chiral Dopant E-1[a]

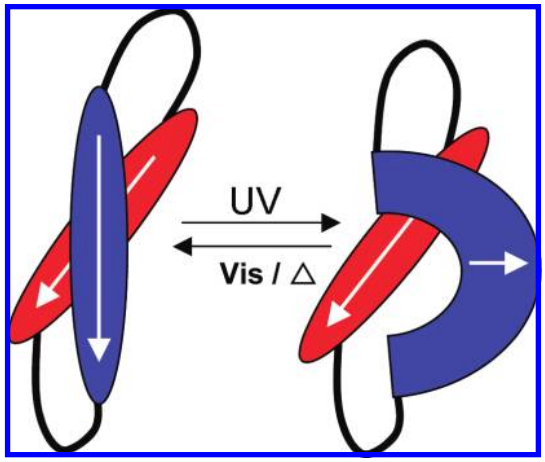

[a] Blue and red structures indicate azobenzene and naphthalene units, respectively.

mainly attributed to the geometrical changes resulting from isomerization of rod shaped *trans* isomer to bent *cis* isomer. In the above conventional design, as the photochromic unit is remotely present from the chiral center, only a weak chiral conformational changes can be achieved by isomerization. In contrast, a greater influence of isomerization of the photochromic unit on both geometrical and chiral conformational changes can be logically expected with our design of azobenzene moiety being an integral part of the rigid chiral core unit.

Results and Discussion

Synthesis and Conformational Analysis. We synthesized the target molecules as a racemic compound in three steps through reduction of the corresponding dinitro compound under dilute conditions.[20] Silica gel column chromatography followed by precipitation from CH_2Cl_2/hexane fetched us the pure *trans* isomer of the racemic compound **E-1**. The NMR and mass spectra supported their structures. The first indication of the absence of free rotation of the naphthalene moiety in **E-1** was provided by ^{1}H NMR studies in solution. A restricted rotation of naphthalene ring within the NMR time scale through the azobenzenophane cavity will make the compound resolvable and allow us to use the different NMR signals of the aliphatic spacer protons as molecular probes for the study of conformational processes. Accordingly, the ^{1}H NMR spectra of **E-1** (300 MHz, 298 K, $CDCl_3$) show three resonances for the bismethylene protons [$-OCH^aH^bCH^c{}_2-$]. This is because the two aliphatic $-OCH^aH^b$ hydrogens become diastereotopic when the exchange of the enantiomers is rendered slow in the NMR time scale. One of the two diastereotopic proton resonance is located at about 4.76 ppm, about 0.16 ppm downfield from its partner. All the four resonances that can be expected from the $-OCH^aH^bCH^cH^d-$ protons of the compound was observed for its *cis* isomer **Z-1**. As expected, there were three resonances observed for the six protons of 1,5-dioxynaphthalene moiety and four resonances for the eight protons of azobenzene unit.

Enantiomeric Resolution. The enantiomers of **E-1** were resolved by semipreparative chiral HPLC (Chiralpak IA column with hexane/EtOAc as an eluent) to give enantiopure (−)**E-1** and (+)**E-1** as first and second fractions ($[\alpha]_D$ (c 0.2, $CHCl_3$) = −204 and +204) respectively. Absorption spectrum of **E-1** and the circular dichroism (CD) spectra of (−)**E-1** and (+)**E-1** were measured in CH_3CN (1.5×10^{-5} M), and the results are shown in Figures 1 and 2, respectively. The UV spectra of **E-1** show maximum absorption in the region of 230 nm (ϵ/M^{-1} cm^{-1} 84340) due to the ^1B_b transition of the naphthalene chromophore. The absorption band at 280−370 nm (λ_{max} = 302 nm, ϵ/M^{-1} cm^{-1} 31 306) corresponds to ^1L_a and ^1L_b transitions of naphthyl group and $\pi-\pi^*$ transition related to azobenzene chromophore. ^1B_b and ^1L_b bands are assigned to the long axis of the naphthyl group, while the ^1L_a band corresponds to the short axis.[21] However, only a weak absorption band for $n-\pi^*$ transition (λ_{max} = 450 nm) is seen in the absorption spectra. In contrast, CD spectra exhibit distinct bands for $\pi-\pi^*$ and $n-\pi^*$ transitions of the azochromophore. The first eluted enantiomer (−)**E-1** shows a negative band for the $n-\pi^*$ transition (λ_{max} = 450 nm) followed by relatively weak CD Cotton effects of a complex patterns between 280 and 370 nm. In the region below 270 nm, the CD spectrum is dominated by a strong positive

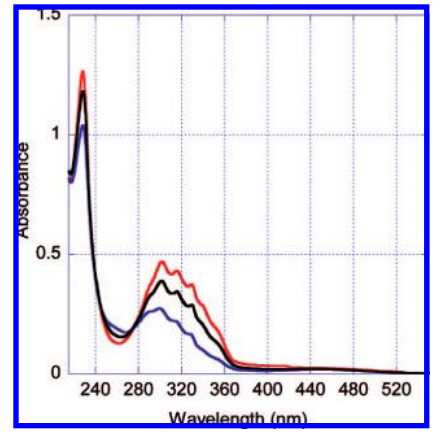

Figure 1. Absorption spectral change of **E-1** in acetonitrile (1.5×10^{-5} M) upon irradiation at room temperature: (a) red line, initial state before irradiation; (b) blue line, photostationary state (PSS) after irradiation at 365 nm; and (c) black line, PSS after irradiation at 436 nm (reverse reaction).

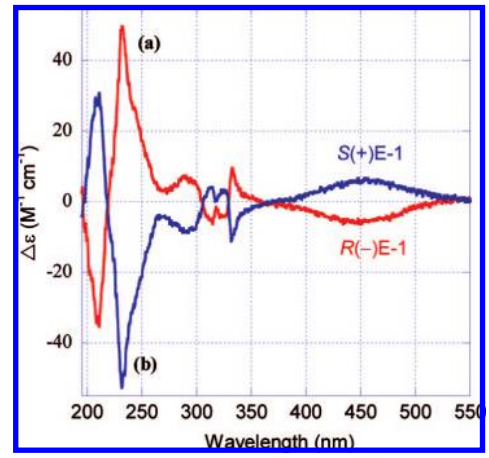

Figure 2. CD spectra of enantiomers of **E-1** in CH_3CN: (a) (−)**E-1** with absolute configuration *R* (red line) and (b) (+)**E-1** with absolute configuration *S* (blue line).

(20) See the Supporting Information.

(21) (a) Di Bari, L.; Pescitelli, G.; Salvadori, P. *J. Am. Chem. Soc.* **1999**, *121*, 7998–8004. (b) Di Bari, L.; Pescitelli, G.; Marchetti, F.; Salvadori, P. *J. Am. Chem. Soc.* **2000**, *122*, 6395–6398.

Table 1. X-ray Structural Data of *trans* **E-1** and Theoretically Calculated Structural Data for *cis* **Z-1**

compound	type	*N*═N (bond lengths, pm)	CNNC	NNCC (angles, deg)	NNC
E-1	Conformer A	1.241	171.2	8.0, −167.9 168.8, −19.3	114.3, 115.1
	Conformer B	1.252	−171.4	16.1, −169.2 −158.9, 25.4	114.8, 113.1
	Conformer C	1.262	−171.8	15.6, −170.0 −159.3, 25.5	112.7, 114.8
Z-1	Calculated[a]	1.249	10.4	41.7, −148.9 55.1, −135.2	125.2

[a] Theoretically calculated data for the lowest energy conformer at the B3LYP/6−31G(d,p) level.

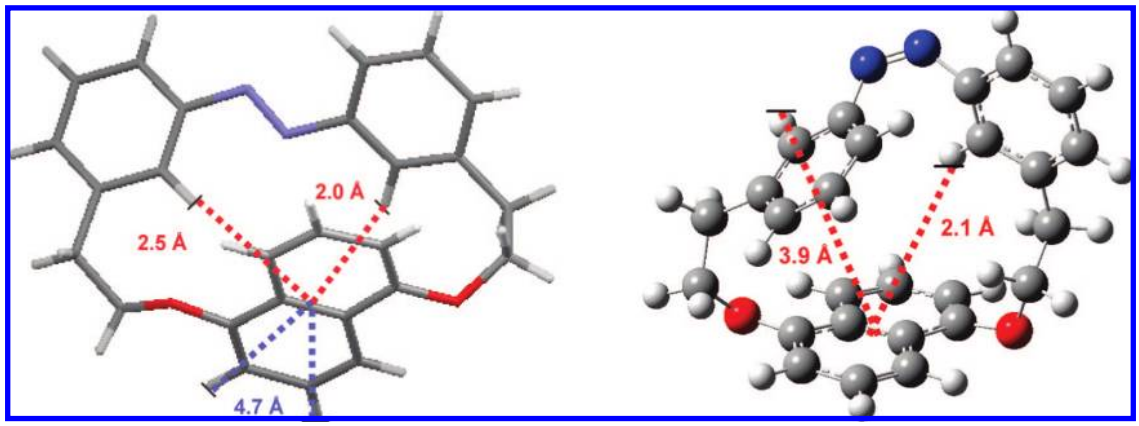

Figure 3. X-ray crystal structure of **E-1** (left) and optimized geometry of its *cis* isomer **Z-1** (right) at the B3LYP/6−31G (d,p) level.

exciton couplet centered at 230 nm due to the ^1B_b long-axis polarized transition of the naphthalene and the B $\pi-\pi^*$ azo transition.[8c] As expected, the second eluted enantiomer (+)**E-1** shows a complete mirror image CD spectrum of its enantiomer (−)**E-1**. By chiral HPLC analysis we confirmed that racemization between the enantiomers (−)**E-1** and (+)**E-1** does not occur in solution even at the elevated temperatures (12 h refluxing in toluene solution).

Structural Properties. The structure of *trans* isomer **E-1** was confirmed by X-ray crystallographic analysis. Single crystals were obtained from a solution of the racemic mixture of **E-1** in CH_2Cl_2 by vapor diffusion with hexane. The space group of the crystal was found to be orthorhombic Pna2(1) with 12 molecules per unit cell. There were three crystallographically independent pairs of enantiomeric molecules, and all of them adopted the C_1 symmetry with slightly different bond lengths, angles, and torsions from each other (Table 1). One of the X-ray crystal structure of **E-1** is shown in Figure 3.[22] The C−*N*═N−C torsion angle of about 171° for all the three conformers indicates that the *trans* azo unit in the molecule deviate from planarity by about 9° due to the ring strain. The B3LYP/6−31G(d,p) optimized structure of *cis* isomer **Z-1** is also shown in Figure 3. The observed deviation in C−*N*═N angle or the C−*N*═N−C dihedral angle for the computationally derived structure of the *cis* isomer (Table 1) from that of *cis* azobenzene[23] point to the evident ring strain in the cyclophane. The *trans* isomer **E-1** was estimated to be more stable than **Z-1** by 16.4 kcal/mol. Analysis of a single crystal of **E-1** by chiral HPLC revealed equal amounts of the enantiomers as a further support to the racemic nature of the crystal. Although we assigned the enantiomers in the X-ray crystal structure with respective *R* and *S* absolute configurations, due to the racemic nature of the crystal we could not correlate them to the corresponding (−)- and (+)-enantiomeric fractions eluted from the chiral column. Resolved enantiomers showed poor tendency for crystallization. It is subsequently difficult to apply the conventional exciton chirality theory, which requires quite accurate knowledge about the orientation of the relevant transition movements.[24] On the other hand, a time-dependent density functional theory (TDDFT) method is now routinely used to assign the absolute configurations of rigid molecules.[25,26] Therefore, to determine the absolute configuration of the enantiomers of **E-1**, we applied the TDDFT method to calculate the electronic CD curve and specific rotations on structure of **E-1** with the *S* configuration for comparison with the experimental ones. On the basis of our calculations,[20] we assigned *S* absolute configuration to the second eluted enantiomer (+)**E-1** and *R* absolute configuration to the first eluted enantiomer (−)**E-1**.

***Trans−Cis* Isomerization and Chiroptical Properties.** After successful resolution of the enantiomers of **E-1**, investigation of their chiroptical properties on photochemical and thermal isomerizations were carried out by UV−vis and CD spectroscopy. Figure 1 shows the absorption changes observed upon

(22) See the Experimental Section and the Supporting Information for details.
(23) Mostad, A.; RØmming, C. *Acta Chem. Scand.* **1971**, *25*, 3561–3568.
(24) (a) *Circular Dichroism: Principles and Applications*; Nakanishi, K., Berova, N., Woody, R. W., Eds.; Wiley-VCH: New York, 2000. (b) Berova, N.; Di Bari, L.; Pescitelli, G. *Chem. Soc. Rev.* **2007**, *36*, 914–931.
(25) (a) Furche, F.; Ahlrichs, R.; Wachsmann, C.; Weber, E.; Sobanski, A.; Vogtle, F.; Grimme, S. *J. Am. Chem. Soc.* **2000**, *122*, 1717–1724. (b) Stephens, P. J.; Devlin, F. J.; Cheeseman, J. R.; Frisch, M. J.; Rosini, C. *Org. Lett.* **2002**, *4*, 4595–4598. (c) Pecul, M.; Ruud, K.; Helgaker, T. *Chem. Phys. Lett.* **2004**, *388*, 110–119. (d) Stephens, P. J.; Devlin, F. J.; Gasparrini, F.; Ciogli, A.; Spinelli, D.; Cosimelli, B. *J. Org. Chem.* **2007**, *72*, 4707–4715.
(26) Rappoport, D.; Furche, F. In *Time-Dependent Density Functional Theory*; Marques, M., Ullrich, C. A., Nogueira, F., Rubio, A., Burke, K., Gross, E. K. U., Eds.; Springer: Berlin, 2006; pp 337−354.

Scheme 1. Photochemical and Thermal Processes Taking Place in ***S*** and ***R*** Enantiomers of Chiroptic Switch Molecule **1**

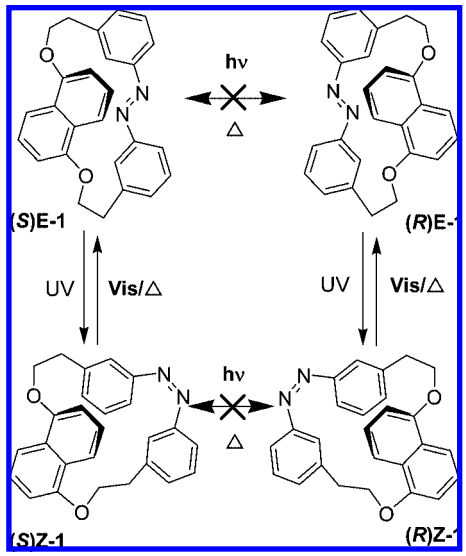

UV and visible light irradiations of **E-1** in acetonitrile solution at 298 K. Upon UV irradiation (λ_{max} = 365 nm), due to photochemical *trans* (**E-1**) to *cis* (**Z-1**) isomerization, there is a gradual decrease seen in the $\pi-\pi^*$ transition bands in the absorption spectra with no concomitant increase in the $n-\pi^*$ band around 450 nm. In the CD spectra of the (***R***)**E-1** and (***S***)**E-1** enantiomers upon irradiation at 365 nm, the $n-\pi^*$ transition gradually becomes more intense whereas the exciton couplet at 230 nm weakens significantly.[20] Furthermore, the two weak exciton couplets between 280 and 370 nm diminish to two weak positive or negative bands for (***R***)**E-1** and (***S***)**E-1**, respectively. These results clearly indicate the substantial influence of the photoisomerization on its chiroptical properties. The photostationary state (PSS) was reached after UV irradiation for about 90 s. Reaction proceeds maintaining isosbestic points through out the irradiation and we determined the ratio of *trans*: *cis* isomers in the PSS_{UV} as 40:60 by HPLC analysis. Any changes of the irradiation wavelength did not enhance the cis ratio in the PSS_{UV}. Upon visible light irradiation (λ_{max} = 436 nm), reverse CD and absorption spectral changes occurred. The PSS_{vis} was obtained in 2 min with 90% of *trans* isomer **E-1**. Alternating irradiations at 365 and 436 nm was repeated several times without any sign of fatigue. The thermal *cis*−*trans* isomerization was determined by monitoring the increase of absorbance at 302 nm in the absorption spectra. The lifetime ($1/k$) of *cis* isomer in the dark at 298 K was found to be about 2.5 h ($k = 1.10 \times 10^{-4}$ s^{-1}), which is much shorter than that of *cis*-azobenzene (4.7 days)[27] but comparable to other strained cyclic azobenzenophanes.[28] The first-order rate plots at different temperatures were used to calculate the activation energy (E_a = 15.1 kcal mol^{-1}) of the thermodynamic back relaxation process. Other thermodynamic parameters such as enthalpy of activation ($\Delta H^{\ddagger}$, 15.7 kcal mol^{-1}) and entropy of activation ($\Delta S^{\ddagger}$, −1.2 cal K^{-1} mol^{-1}) were determined according to Eyring equation.[29] On the basis of the chiral HPLC analysis, we found that the reversible *trans*−*cis* isomerization in (***R***)**E-1** to (***R***)**Z-1** and (***S***)**E-1** to (***S***)**Z-1** proceeds without any racemization. This result reveals that in both **E** and **Z** isomers of **1** the size of the cavity of the cyclophane is not large enough for the free rotation of the naphthalene ring through it. This observation is in agreement with the results obtained by structural analysis of **E-1** and **Z-1** isomers. The minimum through space distance that is required for the free rotation of naphthalene ring was estimated to be about 4.7 Å. Our molecular modeling indicate that the major steric hindrance for the rotation of the naphthalene moiety arise from the hydrogen atoms present at the 2,2′ positions of the azobenzene unit. As shown in Figure 3, the calculated distance from the rotational axis in naphthalene to the sterically hindering hydrogens of azo unit in both the *trans* and *cis* isomers was much shorter than the required 4.7 Å for the free rotation of the naphthalene unit. Scheme 1 summarizes the photoisomerization characteristics of the (***R***)**E-1** and (***S***)**E-1** enantiomers in solution highlighting their photochemically reversible isomerization to (***R***)**Z-1** and (***S***)**Z-1** without undergoing photoinduced racemization.

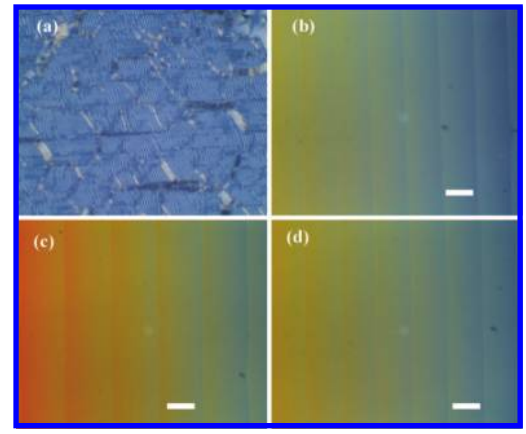

Figure 4. Polarized optical photomicrographs of 0.4 wt% of (***S***)**E-1** dissolved in ZLI-1132 at RT: (a) Chiral nematic fingerprint texture, and reversible change occurring in pitch by irradiation of sample in a wedge type cell evidenced as change in distance between the Cano's lines; (b) before irradiation, (c) PSS_{UV}, (d) PSS_{vis}; scalebar, 150 μm.

Evaluation of Helical Twisting Power. After confirming the chiroptic properties of (***R***)**E-1** and (***S***)**E-1** in solution, we investigated their potential as chirality transfer agents in three commercially available nematic (N) host liquid crystals (LC) of diverse chemical structures namely ZLI-1132, DON-103 and 5CB.[30] The induction of chiral nematic phase was directly evidenced as a fingerprint texture[31] under a polarized optical microscope (Figure 4). Induced helical pitch P for different concentrations of dopant was calculated by well-known Cano's wedge method.[32] The helical sense of the induced N* phase was determined by contact method[33] as well as by measuring the CD spectra (vide infra). Enantiomers of a chiral solute are known to induce an equal but opposite twist in the host N phase.

(27) Asano, T.; Okada, T.; Shinkai, S.; Shigematsu, K.; Kusano, Y.; Manabe, O. *J. Am. Chem. Soc.* **1981**, *103*, 5161–5165.
(28) Bassotti, E.; Carbone, P.; Credi, A.; DiStefano, M.; Masiero, S.; Negri, F.; Orlandi, G.; Spada, G. P. *J. Phys. Chem. A* **2006**, *110*, 12385–12394.
(29) Eyring, H. *Chem. Rev.* **1935**, *17*, 65–77.
(30) (a) ZLI-1132 (TNI = 72.3 °C): Mixtures of 4-(4-alkylcyclohexyl)-benzonitrile and 4-(4-alkylcyclohexyl)-4′-cyanobiphenyl derivatives. (b) DON-103 (TNI = 74.2 °C): Mixtures of cyclohexanoic acid phenyl esters. (c) 5CB (4-cyano-4′-pentylbiphenyl): TNI = 35.0 °C.
(31) *Textures of Liquid Crystals*; Dierking, I., Ed.; Wiley-VCH: Weinheim, 2003.
(32) (a) Solladie, G.; Zimmermann, R. G. *Angew. Chem., Int. Ed. Engl.* **1984**, *23*, 348–362. (b) Sagisaka, T.; Yokoyama, Y. *Bull. Chem. Soc. Jpn.* **2000**, *73*, 191–196.
(33) Isaert, N.; Soulestin, B.; Malthete, J. *Mol. Cryst. Liq. Cryst.* **1976**, *37*, 321–333.

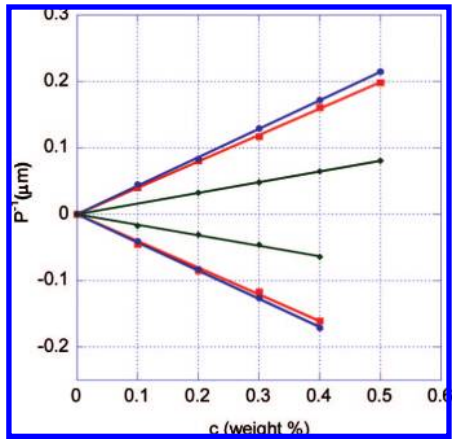

Figure 5. Reciprocal helical pitch as a function of concentration of (***R***)**E-1** and (***S***)**E-1** dopants in 5CB (blue line), ZLI-1132 (red line), and DON-103 (green line) nematic host liquid crystals. Positive and negative P^{-1} values represent right-and left-handed helical twists obtained for (***R***)**E-1** and (***S***)**E-1** respectively.

Table 2. Helical Twisting Powers ($\beta/\mu m^{-1}$) of Dopants in Different Nematic LC Hosts As Determined by Cano's Wedge Method and the Observed Change in Values by Irradiation[a]

		β (μm^{-1})			
dopant	host NLC	initial	PSS_{uv}	PSS_{vis}	$\Delta\beta$ [%][b]
(*R*)E-1	5CB	+43	+36	+40	16
	ZLI-1132	+40	+28	+36	30
	DON-103	+16	+19	+17	19
(*S*)E-1	5CB	−43	−36	−40	16
	ZLI-1132	−40	−28	−36	30
	DON-103	−16	−19	−17	19
(*R*)Z-1[c]	5CB	+36			
	ZLI-1132	+20			
	DON-103	+21			

[a] Positive and negative values represent right- and left-handed helical twists, respectively. [b] Percent change in β observed from initial to UV_{pss}. [c] As determined by HPLC analysis.

Accordingly, chiral dopant (***R***)**E-1** in all the three N host LCs induced a right-handed helix, while a left-handed helix was obtained from (***S***)**E-1**. The inverse of the pitch (P^{-1}) proportionally increased with increase in the concentration of the dopant (Figure 5). The absolute values of β were then determined by plotting P^{-1} against concentration of the dopant and the results are summarized in Table 2. Dopants exhibit moderately high HTP values and their twisting ability in three hosts follows the order 5CB (43 μm^{-1}) ≥ ZLI-1132 (40 μm^{-1}) > DON-103 (16 μm^{-1}). As expected, these dopants with planar chirality exhibit higher β values than that is observed for the photochromic compounds with central chirality (≤10 μm^{-1}) and are comparable to the moderate-to-high helical twisting powers reported for axially chiral photochromic compounds. The two most effective hosts in this work; 5CB and ZLI-1132, have straight and rigid biaryl moieties as part of their mesogenic structure with high longitudinal dipole moment, while the least effective DON-103 is significantly flexible due to ester linkage with dipole moment perpendicular to the molecular long axis. These results are in consistent with the observations that lower conformational freedom and higher structural rigidity of the chiral dopant and the structural similarity between the host and dopant lead to higher HTP values.

Photomodulation of Helical Twisting Power. Next we investigated the effect of isomerization of the dopants on the HTP values. Dopants displayed efficient reversible photoisomerization

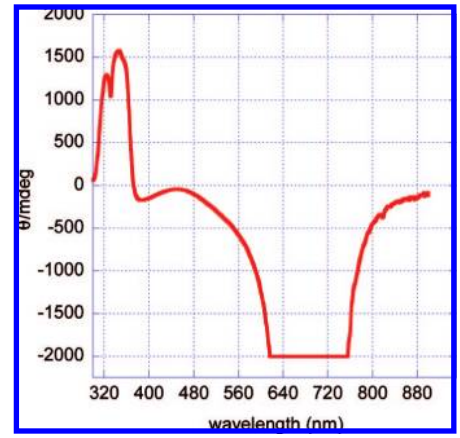

Figure 6. CD spectrum of an induced chiral nematic film having 10% w/w mixture of (***R***)**E-1** in ZLI-1132.

behavior in the LC hosts with UV (λ_{max} = 365 nm) and visible light (λ_{max} = 436 nm) irradiations. In the PSS_{uv}, about 60% conversion of *trans* isomers (***R***)**E-1** and (***S***)**E-1**) to *cis* form (***R***)**Z-1** and (***S***)**Z-1** of the dopants in the host nematic LCs were determined by HPLC analysis. Photoinduced changes in HTP of the dopants were directly evidenced as change in distance between the Cano lines when sample in a wedge cell was observed with a polarized optical microscope under UV or visible light illumination (Figure 4). Variations in the induced pitch and the corresponding HTP values were then calculated using eq 1. It took less than 3 min to reach the photostationary state under UV light illumination. The changes in HTP values obtained by irradiation are given in Table 2. The HTP values of *trans* dopants in 5CB and ZLI-1132 hosts were decreased by UV irradiation. On the contrary, dopants in DON-103 had shown an increase in HTP values with *trans* to *cis* photoisomerization. The process was reversed on illumination with visible light and a PSS_{vis} state in which about 90% of azobenzene units in *trans* form was obtained with in 5 min. From the experimental PSS ratios and the induced helical pitch measurements the absolute values of β for pure *cis* isomer was estimated to be 20 μm^{-1} in ZLI-1132, 36 μm^{-1} in 5CB and 21 μm^{-1} in DON-103. Due to the large difference in helical twisting powers of the *trans* and *cis* isomers in ZLI-1132 (i.e., +40 μm^{-1} for (***R***)**E-1** compared to +20 μm^{-1} for (***R***)**Z-1**), a significant effective change in the induced pitch ca. 28% by alternate UV and visible light irradiations was achieved. We also confirmed that both the *trans* and *cis* isomers of the enantiomers have the same helical twist sense, i.e. right-handed helix for (***R***)**E-1** and (***R***)**Z-1** and left-handed helix for (***S***)**E-1** and (***S***)**Z-1**. Although the decrease in HTP values for the *cis* isomers of the dopants compared to the *trans* isomers in ZLI-1132 and 5-CB can be explained based on the better structural compatibility of the elongated *trans* azo units of the dopants with the host LC molecules, a mechanistic interpretation for the increase in HTP values for the *cis* isomers in DON-103 requires a better understanding of the solvent−solute interactions on the chirality transfer. Because of high twisting ability as well as good phototunability in HTP values of dopants, we employed them for achieving photoaddressable LC films in the visible region.

Photoinduced Modulation of Chiral Nematic Reflection Colors. The reflected colors from chiral nematic phase depends on the helical pitch P of the phase according to the Bragg's law $\lambda_{max} = Pn$, where λ_{max} is the reflection maximum and n is the refractive index of the system. In mixtures of a nematic

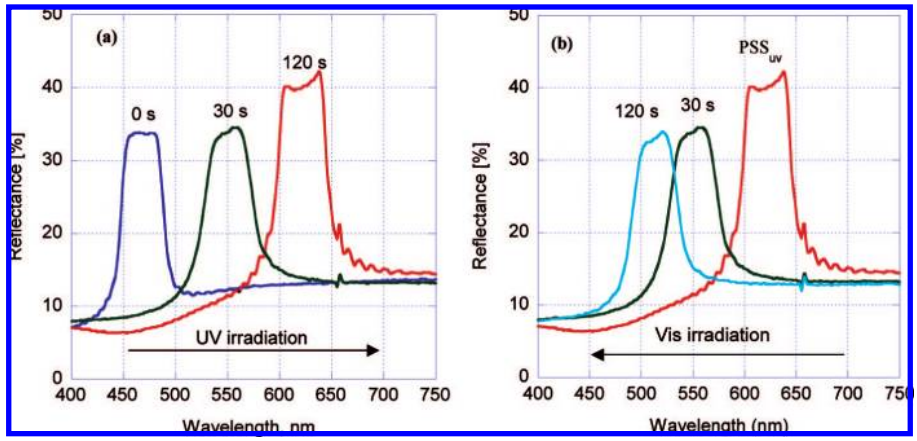

Figure 7. Changes in selective reflection spectra of the chiral nematic LC film consisting of 12 wt% of (***R***)**E-1** in ZLI-1132: (a) on UV irradiation and (b) on visible light irradiation at room temperature.

Figure 8. Changes in reflection color of the chiral nematic LC film consisting of 12 wt% of (***R***)**E-1** in ZLI-1132 by varying UV irradiation time: 0 s (left), 30 s (middle), and 120 s (right).

liquid crystal with a chiral additive, the pitch length can be increased or decreased with concentration of the chiral compound. Therefore, we prepared liquid crystal mixtures with sufficient amount of (***R***)**E-1** and (***S***)**E-1** chiral compounds for the pitch to be in the visible region. Dopants not only have excellent phototunability of helical twisting power due to rigid planar chiral photochromic core structure but also show good miscibility toward the nematic host LCs. A mixture consisting of 10 wt% of (***R***)**E-1** in ZLI-1132 resulted in a reddish LC film. Figure 6 shows its CD spectrum (recorded at normal incidence) having a large negative band corresponding to the selective reflection of the right-handed circularly polarized light (SR-RCPL) in consistent with the right-handedness of the induced chiral nematic phase.[34] A mixture consisting of compound (***R***)**E-1** and ZLI-1132 (12:88 by weight) inside a glass cell consisting of two glass plates coated with polyimide alignment layer with a 5 μm cell gap, showed a chiral nematic phase at room temperature with a selective reflection band around 450 nm. Irradiation with 365 nm light resulted in the shift of the selective reflection band to a longer wavelength red reflection band through green reflection color as shown in Figure 7a and Figure 8. The reflection band returned to the initial state after 3 h in the dark due to thermal *cis* to *trans* isomerization of the azo compound. However, a rapid reversible shift of the reflection color band was achieved by visible-light irradiation as shown in Figure 7b. This process was repeated several times to confirm the fatigue resistance. Thus, a fast reversible photon mode reflection color control with blue, green, and red colors was achieved in an induced chiral nematic film by alternating UV and visible-light irradiation employing the planar chiral dopant with no other auxiliary chiral agents. The reversible blue shift achieved by 436 nm irradiation in this study is about 10 times faster than the switching times reported so far for the thermally driven systems.[8c,14,15] It is true that the change of color in minutes is still too slow for the application to memory or active display media, although it is acceptable for rewritable full-color display media that changes the image several times a day. A further significant improvement in the phototunability of HTP and response times can be achieved by obtaining a higher *trans* to *cis* isomerization ratio at the PSS$_{uv}$ than that is reported here. Therefore studies are in progress to develop more efficient planar chiral photoresponsive dopants with high helical twisting power and faster photo responses.

(34) (a) de Gennes, P. G.; Prost, J. *The Physics of Liquid Crystals*, 2nd ed.; Oxford: New York, 1993. (b) Yoshida, J.; Sato, H.; Yamagishi, A.; Hoshino, N. *J. Am. Chem. Soc.* **2005**, *127*, 8453–8456.

Conclusions

Photochromic compounds having planar chirality were employed to reversibly control the selective reflection colors in an induced chiral nematic liquid crystalline film. For this purpose, a chiral azobenzenophane was designed and synthesized and the enantiomers were resolved by HPLC on a chiral column. These enantiomers showed photochemically reversible isomerization in solution without undergoing thermal or photoinduced racemization. Employing these chiroptic switches as dopants in different host nematic LCs not only exhibit good solubility, reversible photoisomerization with fatigue resistance, and moderately high helical twisting powers but also bring about a large photon mode reversible change in HTP due to *cis*−*trans* isomerization. Furthermore, for the first time, we achieved a fast reversible control of the three primary colors that are both hypsochromically and bathochromically shifted by the action of light in an induced chiral nematic LC film having photo tunable dopant as the only source of molecular chirality. The synthetic achievements and conformational knowledge obtained herein will allow us to design new members of this type of compound with planar chirality and is expected to expand the field of phototunable chiral dopants as well as the chiroptic switches for various applications.

Experimental Section

Instrumentation. ^{1}H and ^{13}C NMR spectra were recorded on a Varian Gemini 300. The chemical shifts are reported in δ (ppm) relative to tetramethylsilane as internal standard. UV−vis spectra were recorded on a JACSO V-570 spectrometer. CD spectra and optical rotations were recorded on a JASCO J-830 spectropolarimeter. High-performance liquid chromatography (HPLC) was

carried out on PD-8020, TOSH with CHIRALPAK IA columns. Matrix-assisted laser desorption ionization time-of-flight mass spectrometry (MALDI-TOF MS) was conducted using an Applied Biosystems Voyager-DE pro instrument operated in reflector mode and samples were prepared through deposition of THF solutions of the compounds and a-cyano-4-hydroxycinnamic acid. Microscopic analyses were performed with an OLYMPUS IMT-2 equipped with a digital camera (CoolPix 995, NIKON) and a Mettler FP82HT hot stage. Photoisomerization was carried out with a superhigh-pressure mercury lamp (500 W, USHIO Inc.) through an appropriate filter (356 or 436 nm).

Materials. Nematic liquid crystal hosts ZLI-1132 and DON-103 were purchased from Merck while 5CB was obtained from TCI chemicals, Japan. Enantiomeric chiral agents, R-1011 (right-handed cholesterics) and S-1011 (left-handed cholesterics) with known helical handedness induction abilities in the above nematic solvents were purchased from Merck. All solvents, reagents and other chemicals were obtained from commercial sources and used without further purification, unless otherwise noted.

Single-Crystal X-ray Diffraction data for E-1: $C_{26}H_{22}N_2O_2$, $F_w = 394.46$, orthorhombic, space group *Pna*2(1), $a = 15.6790(14)$ Å, $b = 9.3310(8)$ Å, $c = 41.624(4)$ Å, $V = 6089.6(9)$ Å^3, $Z = 12$, $\mu = 0.082$ mm^{-1}, T (K) = 183(2), $\rho_{calcd} = 1.291$ mg/m^3, GOF on $F^2 = 1.023$, $R1 = 0.0522$, and $wR2 = 0.1153$ (F^2 all data). Crystal size $0.40 \times 0.30 \times 0.05$ mm^3. Diffraction data were collected on a Bruker Smart Apex diffractometer with Mo Kα radiation. The data reduction was carried out with SAINTPLUS V6.22.[35] Semiempirical absorption correction was applied with SADABS.[36] The structure determination was done with direct methods and refinements with full-matrix least-squares on F^2 with SHELXTL version 6.12.[37]

Measurement of Helical Pitch and Handedness. The chiral nematic liquid crystal was prepared by weighing appropriate amount of host liquid crystal and the dopant into a vial followed by mixing them with the addition of a few drops of dichloromethane. After evaporation of the solvent under reduced pressure, the mixture was loaded into the wedge cell by capillary action at room temperature. The pitch was then determined by measuring the intervals of Cano's lines appearing on the surfaces of wedge-type liquid crystalline cells (EHC, KCRK-07, tan $\theta = 0.0194$). The relationship between the distances of Cano's lines and the helical pitch P is $P = 2R \tan \theta$, where R represents the distance between Cano's lines, and θ is the angle between the cells.

Acknowledgment. This work was supported by a grant-in-aid for science research in a priority area "New Frontiers in Photochromism (No. 471)" from the Ministry of Education, Culture, Sports, Science, and Technology (MEXT), Japan.

Supporting Information Available: Synthesis and characterization data (^{1}H NMR, ^{13}C NMR, HPLC, and X-ray crystallography file of the compound **E-1**), details of computational study. This material is available free of charge via the Internet at http://pubs.acs.org.

JA802472T

(35) *SMART*, version 5.625, and *SAINTPLUS*, version 6.22; Bruker Axs Inc.: Madison, WI, 2000.

(36) Sheldrick, G. M. *SHELXTL*, version 6.12; Bruker AXS: Madison, WI, 2000.

(37) Sheldrick, G. M. *SADABS*; University of Göttingen: Göttingen, Germany, 1996.